

Nuclear-Coulomb interference in π^\pm - ^{16}O scattering

G. S. Mutchler, C. R. Fletcher,* L. V. Coulson,† D. Mann,
N. D. Gabitzsch, and G. C. Phillips
T. W. Bonner Nuclear Laboratories,‡ Rice University, Houston, Texas 77001

B. W. Mayes, E. V. Hungerford, L. Y. Lee, C. Goodman, and J. C. Allred
University of Houston,‡ Houston, Texas 77004
(Received 22 August 1974; revised manuscript received 6 March 1975)

The small angle scattering of π^+ and π^- from ^{16}O has been measured at 155, 185, and 213 MeV laboratory kinetic energy. The real part of the forward scattering amplitude was extracted from the data. The real part extrapolates to zero at 163 ± 3 MeV.

$$\left[\text{NUCLEAR REACTIONS } ^{16}\text{O}(\pi^\pm, \pi^\pm), E=155\text{--}213 \text{ MeV; measured } \sigma(\theta_\pi); \text{ deduced } \text{Ref}_s(0^\circ)/\text{Im}f_s(0^\circ). \right]$$

I. INTRODUCTION

At sufficiently small angles, the elastic scattering amplitudes from the Coulomb and nuclear fields become equal, resulting in a measurable interference term. The magnitude of this term is proportional to the ratio α of the real to the imaginary parts of the hadron-nucleus scattering amplitude. In the case of isoscalar nuclei, the real part of the forward scattering amplitude at 0° (Ref_s) can be extracted from the difference of π^+ and π^- scattering independent of the imaginary part of the forward scattering amplitude at 0° ($\text{Im}f_s$), except for a small model dependent correction term. Knowledge of the Ref_s is necessary in checking the dispersion relations¹ and the validity of various theoretical models describing pion-nucleus scattering. A knowledge of the Ref_s is also required in the analysis of pion total cross section measurements.²

This experiment determines the Ref_s for π^\pm - ^{16}O elastic scattering by measuring the small angle differential cross section at laboratory angles from 4° to 11° . The pion laboratory kinetic energies, 155, 180, and 213 MeV, were chosen to span the pion-nucleon ($\frac{3}{2}, \frac{3}{2}$) resonance, where the Ref_s vanishes.

II. EXPERIMENTAL ARRANGEMENT

The experimental arrangement is shown in Fig. 1. The 600 MeV external proton beam from the synchrocyclotron at the Space Radiation Effects Laboratory (SREL) was used to generate a variable energy pion beam. A $\pm 2\%$ momentum bite was provided by slits placed in the external pion channel. A two meter CO_2 gas Čerenkov detector (at atmospheric pressure) rejected electrons. Protons in the π^+ beam were removed by a thin

degrader placed at the momentum slit. The scattering target was a 12 cm diameter water cell 1.05 g/cm^2 thick with 8 mg/cm^2 Mylar windows.

The recoil protons from the water and slow ($\beta < 0.7$) reaction products from the ^{16}O , such as (π^+ , $2p$), were identified by their pulse height in the plastic scintillator S_2 and subtracted from the data. The scattered beam was not magnetically analyzed; therefore, inelastically scattered pions were not rejected. The beam was restricted to a $4 \text{ cm} \times 4 \text{ cm}$ square by the multiwire proportional chambers X3-Y3. Computer dead time limited useful beam intensities to less than $1000 \pi/\text{sec}$.

The (x, y) coordinates of the π^\pm incoming and outgoing trajectories were measured using six two-dimensional multiwire proportional counters (MWPC). The MWPC's were placed directly in the pion beam. The smallest scattering angle for which the cross section was analyzed ($\sim 4\text{--}5^\circ$) was determined by Coulomb multiple scattering of the beam in the target. The largest angle ($\sim 10^\circ$) was determined by the size of the last MWPC plane ($28 \text{ cm} \times 28 \text{ cm}$). When the system was triggered by a fast coincidence between the plastic scintillators placed before and after the MWPC's, the wire number of each coordinate was read out digitally and fed into an IBM 360/44 on-line computer. Details of the MWPC's and readout electronics have been published elsewhere.³

Straight line fits to the three (x, y) coordinates of the incident and the scattered pions were performed. The scattering angle θ was calculated from $\cos\theta = \hat{r}_1 \cdot \hat{r}_2$, where \hat{r}_1 and \hat{r}_2 are unit vectors in the directions of the incoming and outgoing trajectories, respectively. The intersections of these lines with the target plane were required to be less than 5 mm apart. This criterion allows a tenfold reduction in the decay muons accepted by

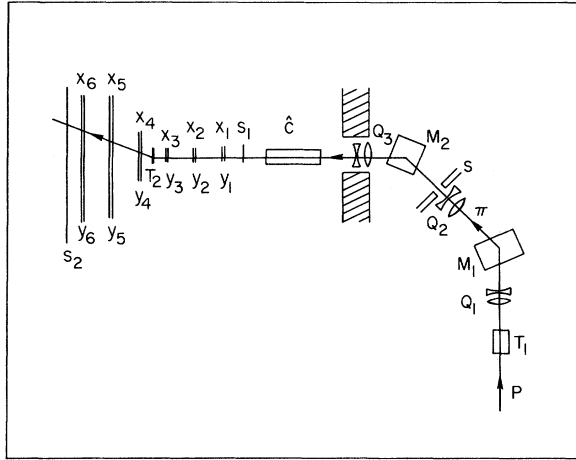


FIG. 1. Experimental setup. Pions are produced at target T_1 . Magnets M_1 and M_2 bend the secondary pion beam into the target room, while quadrupole magnets Q_1 , Q_2 , and Q_3 focus the beam on the scattering target T_2 . The slits S near Q_2 define the beam momentum. MWPC's X_1 - X_6 and Y_1 - Y_6 measure the particle trajectories, and scintillators S_1 and S_2 provide fast logic signals. The CO_2 threshold Čerenkov detector (\hat{C}) electronically removes electrons from the beam.

the system by limiting the effective decay length to ± 5 cm from the target. The muons from the decay $\pi^\pm \rightarrow \mu^\pm + \nu$ in the target-out data provided a convenient method of measuring the beam momentum and purity.⁴ The beam parameters are listed in Table I.

TABLE I. Beam purity.

T_π	$\% \pi^+$ ^a	$\% \pi^-$	$\% e^-$ ^b	$\% \mu^-$ ^c
155	84	53	42	9
180	90	66	29	7
213	95	77	20	5

^a Čerenkov counter not used; therefore, beam contains e^+ and μ^+ . Protons rejected by absorber and dE/dx .

^b Percentage of particles tagged as electrons by the Čerenkov counter.

^c Percentage of particles passed by Čerenkov counter that were not pions.

III. DATA ANALYSIS

Figure 2 shows the π^\pm - ^{16}O differential cross sections. The π^+ data were taken at 159, 185, and 213 MeV, while the π^- data were taken at 155, 180, and 213 MeV. The data have been corrected for the Coulomb scattering of the μ^\pm beam contaminants. The differential cross sections in the c.m. system are given in Table II.

The proton background [proton recoils, $^{16}\text{O}(\pi, 2p)$, etc.] was approximately 100 mb/sr for π^+ scattering and 20 mb/sr for π^- scattering. The $p(\pi^\pm, \pi^\pm)p$ cross sections were calculated from the phase shifts of Roper and Wright.⁵ The cross sections were transformed from the π -nucleon c.m. system to the π -nucleus c.m. system and subtracted from the data. The target-out data (decay muons) were convolved with a Gaussian to simulate multiple scattering in the target. Details of this calcu-

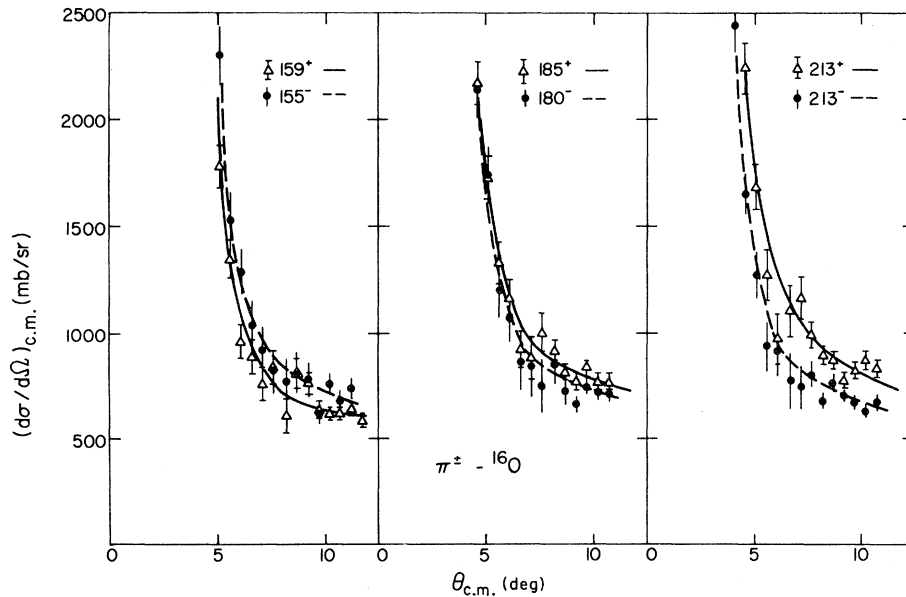


FIG. 2. The small angle differential cross section for π^\pm - ^{16}O elastic scattering. The curves are fits to the data using Eq. (13) and the parameters given in Table II (see text).

TABLE II. π^\pm - ^{16}O differential cross section. Angles and cross sections are given in the c.m. system.

$\theta_{\text{c.m.}}^*$ (deg)	$\frac{d\sigma^+}{d\Omega_{\text{c.m.}}}$ (b)	$\Delta \frac{d\sigma^+}{d\Omega_{\text{c.m.}}}$ (b)	$\frac{d\sigma^-}{d\Omega_{\text{c.m.}}}$ (b)	$\Delta \frac{d\sigma^-}{d\Omega_{\text{c.m.}}}$ (b)
Pion kinetic energy (lab)=159 MeV for π^+ and 155 MeV for π^-				
5.1	1.784	0.099	2.298	0.138
5.6	1.349	0.093	1.531	0.126
6.1	0.961	0.083	1.290	0.115
6.6	0.890	0.080	1.038	0.108
7.1	0.759	0.080	0.923	0.107
7.6	0.841	0.084	0.833	0.109
8.2	0.611	0.082	0.773	0.111
8.7	0.812	0.073	0.809	0.101
9.2	0.760	0.054	0.786	0.078
9.7	0.639	0.038	0.617	0.054
10.2	0.621	0.033	0.762	0.048
10.7	0.617	0.031	0.683	0.044
11.2	0.642	0.032	0.736	0.049
Pion kinetic energy (lab)=185 MeV for π^+ and 180 MeV for π^-				
4.6	2.171	0.104	2.116	0.239
5.1	1.729	0.098	1.742	0.133
5.6	1.332	0.096	1.205	0.130
6.1	1.156	0.093	1.068	0.128
6.6	0.914	0.094	0.859	0.132
7.1	0.871	0.096	0.842	0.137
7.7	0.995	0.090	0.753	0.134
8.2	0.913	0.064	0.850	0.102
8.7	0.803	0.045	0.718	0.063
9.2	0.765	0.037	0.663	0.044
9.7	0.835	0.037	0.749	0.042
10.2	0.763	0.035	0.719	0.042
10.7	0.764	0.034	0.713	0.044
Pion kinetic energy (lab)=213 MeV for π^\pm				
4.1	3.314	0.145	2.441	0.129
4.6	2.245	0.117	1.651	0.105
5.1	1.685	0.114	1.266	0.108
5.6	1.278	0.119	0.935	0.116
6.1	0.978	0.119	0.915	0.122
6.6	1.105	0.122	0.773	0.127
7.2	1.165	0.102	0.739	0.101
7.7	1.000	0.064	0.797	0.061
8.2	0.895	0.047	0.680	0.039
8.7	0.883	0.043	0.760	0.036
9.2	0.782	0.039	0.698	0.033
9.7	0.829	0.040	0.671	0.032
10.2	0.877	0.042	0.635	0.032
10.7	0.837	0.043	0.670	0.036

lation are given in Ref. 4.

The data were fitted using a formalism due originally to Bethe.⁶ The scattering amplitude is separated in terms of the Coulomb amplitude F_C and a remainder F_{CN} , which is the strong amplitude modified by the Coulomb phase. The differ-

ential cross section is given by

$$\frac{d\sigma}{d\Omega} = |F_C + F_{CN}|^2. \quad (1)$$

Bethe assumed that both the nuclear and Coulomb phase shifts were small. Knowing that the Coulomb phase shift is a slowly varying function of the impact parameter, he obtained the following approximation valid for small momentum transfers and not too strong Coulomb fields:

$$F_{CN} = f_s e^{i\phi_B}, \quad (2)$$

where ϕ_B is the Coulomb phase averaged over all impact parameters. Then the differential cross section is given by

$$\frac{d\sigma}{d\Omega} = \left| -\eta \frac{2p}{|t|} G(t) + f_s(t) e^{-i(\phi_C - \phi_B)} \right|^2, \quad (3)$$

where the Coulomb phase is given by

$$\phi_C = -2\eta \ln(\sin\theta^*/2) + 2 \arg \Gamma(1 + i\eta). \quad (4)$$

In the above equations k is the laboratory momentum of the pion, $|t| = -2k^2(1 - \cos\theta^*)$ is the usual squared four-momentum transfer, $\eta = Ze^2/\hbar c\beta$, $G(t)$ is the electromagnetic form factor of the nucleus and the pion, and k^* and θ^* are in the c.m. system. The phase difference $2\phi = \phi_C - \phi_B$ was taken from West and Yennie⁷:

$$2\phi = -2\eta \ln(\sin\theta^*/2) - \eta \times \int_{-4k^2}^{\infty} \frac{dt'}{|t' - t|} \left[1 - \frac{f_s(t')}{f_s(t)} \right]. \quad (5)$$

A Gaussian charge form factor $G(t) = \exp[-\frac{1}{6}(R_0^2 + R_\pi^2)|t|]$ was used with $R_\pi = 0.8$ fm as the rms charge radius of the pion and $R_0 = 2.71$ fm as the rms charge radius of the ^{16}O nucleus.⁸ A phenomenological expression was used for the strong amplitude⁹:

$$F_s = \frac{k\sigma_{\text{tot}}}{4\pi} [i + \alpha(0^\circ)] \exp[-\frac{1}{6}R_s^2|t|]. \quad (6)$$

The strong interaction radius was taken to be equal to the charge radius. Because of the limited angular range covered by the data, it was not considered necessary to allow the nuclear phase to vary with $|t|$ as is done in Ref. 9.

From total cross section data it is known that large π^\pm differences $(\sigma_{\text{tot}}^+ - \sigma_{\text{tot}}^-)/\frac{1}{2}(\sigma_{\text{tot}}^+ + \sigma_{\text{tot}}^-) \approx 10\%$, which are not accounted for by Eq. (3), exist for self-conjugate nuclei.^{2,10} These differences are due primarily to the distortion and energy shift at the nuclear surface of the pion wave function by the Coulomb field of the nucleus. Fäldt and Pilkuhn^{11,12} have estimated these effects using a semiclassical model in which the pion trajec-

tories are taken to be hyperbolic orbits and the nucleus is represented as a black disc of radius R . They find that the measured cross sections can be related to the "true" strong interaction cross sections evaluated at the energy of the pion at the nuclear surface E_R , but corrected by a Coulomb flux factor. The flux factor arises because, due to the attraction or repulsion of the pions, the nucleus appears to have a radius $R(\pi^\pm) = R/(1 + \delta)$. Specifically,

$$\delta = Z_\pi Z_N \alpha E / k^2 R, \quad (7)$$

$$E_R = E - Z_\pi Z_N \alpha / R, \quad (8)$$

$$k_R = k / (1 + \delta), \quad (9)$$

$$\sigma_M = \sigma_s / (1 + \delta)^2, \quad (10)$$

$$t_R = t / (1 + \delta)^2, \quad (11)$$

where E is the total laboratory energy and k is the laboratory momentum of the incident pion. σ_M is the measured (charge dependent) total cross section and σ_s is the "true" charge independent total cross section. α is the fine structure constant. Z_π and Z_N are the charge of the pion and nucleus.

Therefore, Eq. (3) is modified to read¹²

$$\frac{d\sigma}{d\Omega} = \left| F_C(k_R, t_R) + \frac{1}{1 + \delta} f_s(k_R, t_R) e^{-2i\phi} \right|^2, \quad (12)$$

$$\frac{d\sigma}{d\Omega} = \left| -\eta \frac{2k(1 + \delta)}{|t_R|} G(t_R) + \frac{ke^{-2i\phi}}{(1 + \delta)^2} \frac{\sigma_s}{4\pi} [i + \alpha(0^\circ)] \exp(-\frac{1}{6} R_s^2 |t_R|) \right|^2. \quad (13)$$

In this model α should be independent of the pion charge. Notice that the main correction term comes from the kinematic factor $\sigma_s / (1 + \delta)^2$. Therefore, using Eqs. (3) and (6) with $\sigma_M \approx \sigma_s / (1 + \delta)^2$, as is done in Refs. 9 and 13, will give approximately the same value of α as Eq. (13).

Table III gives the values of $\alpha(0^\circ)$ and the $\text{Re}f_s$ obtained by fitting Eq. (13) to the data. The only free parameter was α . The total cross sections were obtained by fitting the published data of Refs. 14 and 15 with a third order polynomial:

$$\sigma_M = [a_0 + a_1 x + a_2 x^2], \quad (14)$$

where

$$a_0 = 834 \pm 11, \quad a_2 = -0.032 \pm 0.008,$$

$$a_1 = -1.0 \pm 0.4, \quad x = T_\pi - 155 \text{ MeV}.$$

A best straight line fit to the values given in Table III extrapolates to $\alpha^+ = 0$ at $T_\pi = 186 \pm 9$ MeV and α^-

$= 0$ at $T_\pi = 147 \pm 8$ MeV. Thus $\text{Re}f_s$ would appear to be charge dependent, contrary to the assumptions of the model. Such a result would disagree with the results for π^\pm -¹²C of Refs. 9 and 13 where the $\text{Re}f_s$ was found to be consistent with charge independence within experimental errors.

The value of α is very sensitive to the value of σ_s used in the fit. Thus a possible explanation for the charge dependence of $\text{Re}f_s$ is a normalization error in the differential or total cross sections. Assuming that $\alpha^+ = \alpha^-$, $\text{Re}f_s$ can be extracted from the difference of the π^+ and π^- data independent of σ_s , except for a small correction term. The laboratory energies must be chosen so that the π^\pm energies and momenta at the nuclear surface are equal; that is, $E_R^+ = E_R^- = E_R$ and $k_R^+ = k_R^- = k_R$. This requires that

$$E^+ = E_R + Z_k \alpha / R, \quad (15a)$$

$$E^- = E_R - Z_k \alpha / R, \quad (15b)$$

TABLE III. Forward nuclear scattering amplitude parameters for π^\pm -¹⁶O. The data were fitted with Eq. (13) allowing α to vary. $\text{Re}f_s$ and $\text{Im}f_s$ are evaluated in the laboratory system. To convert to the c.m. system multiply by $k_{c.m.}/k_{\text{lab}}$.

	T_π (MeV)	E_R (MeV)	σ_s (mb)	$\alpha(0^\circ)$	χ^2/n	$\text{Re}f_s(0^\circ)$ (fm)	$\text{Im}f_s(0^\circ)$ (fm)
π^-	155	298	825 ± 12	-0.02 ± 0.03	0.94	-0.16 ± 0.31	8.72 ± 0.13
	180	323	791 ± 9	-0.15 ± 0.04	0.69	-1.40 ± 0.41	9.31 ± 0.10
	213	356	726 ± 13	-0.22 ± 0.02	1.90	-2.09 ± 0.33	9.51 ± 0.25
π^+	159	296	825 ± 12	0.13 ± 0.02	1.10	1.13 ± 0.38	8.72 ± 0.13
	185	321	791 ± 9	-0.02 ± 0.02	1.36	-0.16 ± 0.37	9.31 ± 0.10
	213	349	738 ± 13	-0.10 ± 0.02	1.56	-0.93 ± 0.36	9.67 ± 0.25

and leads to

$$F_C^+(k_R, t_R) = -F_C^-(k_R, t_R) \equiv F_C, \quad (16a)$$

$$f_s^+(k_R, t_R) = f_s^-(k_R, t_R) \equiv f_s, \quad (16b)$$

$$\phi^+ = -\phi^- \equiv \phi; \quad (16c)$$

then, from Eq. (12) and Eq. (16),

$$\begin{aligned} \frac{d\sigma^+}{d\Omega} - \frac{d\sigma^-}{d\Omega} &= 4F_C \cos 2\phi \text{Re}f_s \\ &- 4|\delta| [(\text{Im}f_s)^2 - (\text{Re}f_s)^2 + F_C \sin 2\phi \text{Im}F_s]. \end{aligned} \quad (17)$$

In the angular region covered by the data $2\phi \sim 180^\circ$ and $|\delta| \text{Re}f_s \ll F_C$. Therefore, Eq. (17) reduces to

$$4F_C \text{Re}f_s \cong \frac{d\sigma^+}{d\Omega} - \frac{d\sigma^-}{d\Omega} + 4|\delta| \frac{k^2 \sigma_s^2}{16\pi^2} \exp[-\frac{1}{3}R_s^2 |t_R|], \quad (18)$$

where we have used Eq. (6) to evaluate $\text{Im}f_s$.

Although Eq. (18) still contains σ_s , it appears in a correction term, multiplied by δ which is of the order of 0.05. Of course we have replaced the problem of normalizing the differential and total cross section data with one of normalizing the π^+

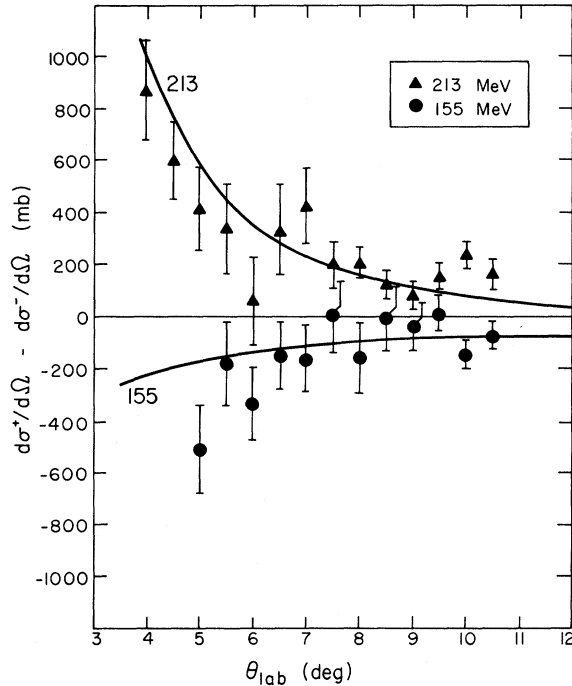


FIG. 3. The difference of the π^+ - and π^- - ^{16}O small angle elastic scattering versus θ_{lab} at 155 and 213 MeV. The solid curves are calculated from Eq. (18) using the parameters given in Table IV (see text). The 180 MeV data points are all near zero and were not plotted to emphasize the 155–213 MeV difference.

TABLE IV. Forward nuclear scattering amplitude parameters for π^\pm - ^{16}O . Parameters were obtained by fitting $(d\sigma^+/d\Omega) - (d\sigma^-/d\Omega)$ with Eq. (18) (see text).

T_π (MeV)	σ_s (mb)	$\text{Re}f_s(0^\circ)$ (fm)	χ^2/n	$\alpha(0^\circ)$
157.0	825 ± 12	0.24 ± 0.17	0.71	0.03 ± 0.02
182.5	791 ± 9	-0.69 ± 0.19	0.65	-0.07 ± 0.02
213.0	732 ± 13	-1.53 ± 0.19	1.54	-0.16 ± 0.01

and π^- differential cross section data. However, the former requires the absolute normalization of all three sets of data to be correct, while the latter depends primarily on the relative normalization of the π^+ and π^- data. Furthermore, analyzing the difference has other advantages. The inelastic events cancel to first order. Also, the value of the $\text{Re}f_s$ extracted is insensitive to the exact shape of the data. This is particularly important because of the anomalies in the angular distributions caused by the muon background. These anomalies increase the χ^2 per degree of freedom by about 0.5 for the π^+ data.¹⁶

The differences were fitted with Eq. (18) using the values of σ_s given in Table III. (All terms were retained for the fit.) The results are given in Table IV and Fig. 3. The real part vanishes at $T_\pi = 163 \pm 3$ MeV in agreement with the carbon data. The error bars on the data points of Fig. 3 are statistical errors only. The errors quoted for $\text{Re}f_s$ in Table IV (and for α^\pm in Table III) were obtained by varying $\text{Re}f_s$ (or α^\pm) until the χ^2 increased by one.

These results can be checked by fitting the data with Eq. (13) using the values of α from Table IV and allowing σ_s to vary. The results are given in Table V. The $\text{Re}f_s$ can be made charge independent by renormalizing the total cross section data

TABLE V. Values of σ_s derived from the requirement $\alpha^+ \equiv \alpha^-$. The data were fitted with Eq. (13), allowing σ'_s to vary. The values of α were taken from Table III. The last column gives the ratio of the fitted value of the total cross section, σ'_s , to the measured value σ_s from Table III.

	T_π (MeV)	$\alpha(0^\circ)$	σ'_s (mb)	χ^2/n	σ'_s/σ_s
π^-	155	0.03 ± 0.02	802 ± 10	0.99	0.97
	180	-0.07 ± 0.02	765 ± 8	0.63	0.97
	213	-0.16 ± 0.01	691 ± 5	0.48	0.95
π^+	159	0.03 ± 0.02	802 ± 10	2.14	0.97
	185	-0.07 ± 0.02	780 ± 8	1.93	0.99
	213	-0.16 ± 0.01	720 ± 5	2.05	0.98

by 0.97, or the differential cross section data by 1.04. The problem of large χ^2/n for the π^+ data still remains. Although χ^2 is increased by the shape anomalies caused by the muon background, the minimum in χ^2 occurs at a much larger σ_s than for the π^- data. This is due to the shape of the angular distribution, not the normalization. The large background due to the $\pi^+ - p$ scattering may be responsible for this shape distortion.

IV. DISCUSSION AND CONCLUSIONS

The zero of the Ref_s would occur at the (3, 3) resonance energy for π -nucleon scattering, provided all other partial waves were negligible. In fact, the tail of the $T = \frac{1}{2}$, $J = \frac{3}{2}$ resonance at 611 MeV causes the zero of the Ref_s for $\pi^- - p$ scattering to occur about 10 MeV higher than for $\pi^+ - p$ scattering.¹⁷ Similarly, in the case of π -nucleus scattering, other partial waves may contribute a sizable nonresonant background, so that the zero of the Ref_s does not necessarily occur at the π -nucleon resonance energy.¹⁸

It should also be noted that the position of the maximum of $Imf(0^\circ)$ in the π -nucleus system is not well known. The peak of the total cross section is shifted downward in energy by about 50 MeV.^{2,10,14,15,19} However, since $\sigma_{tot} = 4\pi Imf(0^\circ)/k$, the peak of σ_{tot} will always be at an energy lower than the energy at which $Imf(0^\circ)$ peaks. For example, the (3,3) resonance in π -nucleon scattering occurs at 190 MeV, but the total cross section peaks at about 175 MeV.²⁰ Since the bump in the π -nucleus excitation curve is considerably broader than in the π -nucleon system, the total cross section peak has a large downshift. This can be seen in the data of Wilkin *et al.*,² where σ_{tot} for ^{12}C and ^{32}S peak at 140 MeV or lower, while the Imf_s peaks at 190 MeV or higher.

The Ref_s can be calculated from forward pion-nucleon dispersion relations containing integrals over Imf_s (and hence σ_{tot}).¹ Such calculations have been made for π - ^{12}C scattering^{9,22} and indicate that Ref_s has a zero near 160 MeV, in agreement with the experimental results of Refs. 9 and 13. These calculations are not available for ^{16}O due to the lack of σ_{tot} data at higher energies. The Ref_s can be calculated from models of π -nucleus scattering. Various authors²³ make use of optical potentials, Glauber approximations, the concept of the index of refraction, the concept of doorway states, or deal directly with a multiple scattering series. All of these workers have some success

at predicting the position of the energy of the total cross section peaks, but give varying predictions for the zero of the Ref_s . Most of these papers do not give numerical predictions for the zero of the Ref_s for ^{16}O . Glauber theory predicts that the zero will occur at the π -nucleon resonance energy (190 MeV). Some authors^{24,25} predict a sizable shift in the zero depending on the form used for extrapolating the π -nucleon scattering amplitude off-shell. Other authors^{18,26} find a substantial effect due to the presence of a nonresonant background. It is probable that the position of the zero is due to a number of effects acting together in a complicated way.

An extensive amount of work has been done on optical potentials, mostly on π - ^{12}C scattering. Most authors give their results for σ_{tot} , but not for Ref_s . Dedonder²⁷ finds that the zero of the Ref_s varies from 100 to 150 MeV for π - ^{12}C depending on the form used for the off-energy shell pion-nucleon scattering. Phatak, Tabakis, and Landau²¹ predict $Ref_s = 0$ at 156 MeV with a slope at zero of -0.049 fm/MeV for π - ^{16}O scattering. This compares well with the present results of 163 ± 3 MeV and a slope of -0.031 ± 0.003 fm/MeV. They overestimate the total cross section by about 100 mb at the peak, which could account for the greater slope that they predict.

In conclusion, the real part of the forward scattering amplitude was extracted from the small angle differential elastic scattering of π^\pm from ^{16}O . Using published total cross sections, the resulting values for Ref_s were charge dependent with the zero of Ref_s^+ occurring at $T_\pi = 186 \pm 9$ MeV and of Ref_s^- occurring at $T_\pi = 147 \pm 8$ MeV. A charge independent value of Ref_s was calculated from the differences of the small angle differential cross sections. The two results could be reconciled by a 3-4% relative renormalization of the two sets of data. Using the difference between π^+ and π^- data, the Ref_s extrapolates to zero at $T_\pi = 163 \pm 3$ MeV, in reasonable agreement with the π^\pm - ^{12}C data and the optical model predictions of Phatak *et al.*²¹

ACKNOWLEDGMENTS

We would like to express our gratitude to Dr. Robert Siegel, W. P. Madigan, and the entire staff of the Space Radiation Effects Laboratory for their support and cooperation. We would also like to thank Mr. Kenneth Hogstrom for his participation in this experiment.

- *Present address: Houston Aerospace Systems Division, National Aeronautics and Space Administration, Houston, Texas.
- †Present address: Radiation Physics Department, National Accelerator Laboratory, P.O. Box 500, Batavia, Illinois 60510.
- ‡Work supported in part by the U. S. Atomic Energy Commission.
- ¹T. E. O. Ericson and M. F. Locher, Nucl. Phys. A148, 1 (1970).
- ²C. Wilkin, C. R. Cox, J. J. Domingo, K. Gabathuler, E. Pedroni, J. Rohlin, P. Schwaller, and N. W. Tanner, Nucl. Phys. B62, 61 (1973).
- ³J. Buchanan, L. V. Coulson, N. Gabitzsch, E. V. Hungerford, G. S. Mutchler, R. Persson, M. L. Scott, J. Windish, and G. C. Phillips, Nucl. Instrum. Methods 99, 159 (1972).
- ⁴L. V. Coulson, C. R. Fletcher, E. V. Hungerford, G. S. Mutchler, G. C. Phillips, M. L. Scott, J. C. Allred, C. Goodman, and B. W. Mayes, Nucl. Instrum. Methods 101, 247 (1972); and M. L. Scott, Ph.D. thesis, 1972, Rice University (unpublished).
- ⁵L. D. Roper and R. M. Wright, Phys. Rev. 138, B190 (1965).
- ⁶H. A. Bethe, Ann. Phys. 3, 190 (1958).
- ⁷C. B. West and D. R. Yennie, Phys. Rev. 172, 1413 (1968).
- ⁸H. R. Collard, L. R. B. Elton, and R. Hofstadter, in *Landolt-Börnstein Zahlenwerte und Funktionen aus Naturwissenschaften und Technik, New Series*, edited by H. Schopper (Springer-Verlag, Berlin, 1967), Vol. 2, p. 34.
- ⁹F. Binon, V. Bobyn, P. Duteil, N. Gouanere, L. Hugon, J. P. Pergneux, J. Renuart, S. Schmit, M. Spighel, and J. P. Stroot, Nucl. Phys. B33, 42 (1971); B40, 608 (1972).
- ¹⁰A. S. Clough, G. K. Turner, B. W. Allardyce, C. J. Batty, J. D. McDonald, R. A. J. Riddle, L. H. Watson, M. E. Cage, G. J. Pyle, and G. T. A. Squier, Phys. Lett. 43B, 476 (1973).
- ¹¹G. Fäldt and H. Pilkuhn, Phys. Lett. 40B, 613 (1972).
- ¹²G. Fäldt and H. Pilkuhn, Phys. Lett. 46B, 337 (1973).
- ¹³G. S. Mutchler, M. L. Scott, C. R. Fletcher, E. V. Hungerford, L. V. Coulson, N. D. Gabitzsch, G. C. Phillips, B. W. Mayes, L. Y. Lee, J. C. Allred, and C. Goodman, Phys. Rev. C 9, 1198 (1974).
- ¹⁴B. W. Allardyce, C. J. Batty, D. J. Baugh, W. J. McDonald, R. A. J. Riddle, L. H. Watson, M. E. Cage, G. J. Pyle, G. T. A. Squier, A. S. Clough, and G. K. Turner, Rutherford Laboratory HEP Division Journal Report No. RL-73-038 (unpublished).
- ¹⁵N. D. Gabitzsch, G. S. Mutchler, C. R. Fletcher, E. V. Hungerford, L. Coulson, D. Mann, T. Witten, M. Furić, G. C. Phillips, B. Mayes, L. Y. Lee, J. Hudomalj, J. C. Allred, and C. Goodman, Phys. Lett. 47B, 234 (1973); N. D. Gabitzsch, Ph.D. thesis, Rice University, 1973 (unpublished).
- ¹⁶The anomalies appear to be worse for the π^+ data than for the π^- data. The reason for this is not known.
- ¹⁷G. Höhler, G. Ebel, and J. Giescke, Z. Phys. 180, 430 (1964).
- ¹⁸L. S. Kisslinger and W. L. Wang, Phys. Rev. Lett. 30, 1071 (1973).
- ¹⁹F. Binon, P. Duteil, J. P. Gasson, J. Gorres, L. Hugon, J. P. Pergneux, S. Schmit, M. Spighel, and J. P. Stroot, Nucl. Phys. B17, 1681 (1970).
- ²⁰A. A. Carter, J. K. Williams, D. V. Bugg, P. J. Bussey, and D. R. Dance, Nucl. Phys. B26, 445 (1971).
- ²¹S. C. Phatak, F. Tabakis, and R. H. Landau, Phys. Rev. C 7, 1803 (1973).
- ²²C. J. Batty, G. T. A. Squier, and G. K. Turner, Nucl. Phys. B67, 492 (1973).
- ²³It would be impractical to list all the recent works dealing with π -nucleus scattering. Instead we refer the reader to the review given by C. Wilkin at the Fifth International Conference on High Energy Physics and Nuclear Structure held at Uppsala, June, 1973 [*High Energy Physics and Nuclear Structure*, edited by G. Tibell (North-Holland, Amsterdam/American Elsevier, New York, 1974); M. M. Sternheim and R. R. Silbar, Annu. Rev. Nucl. Sci. (to be published)].
- ²⁴T. E. O. Ericson and J. Hüfner, Phys. Lett. 33B, 601 (1970).
- ²⁵R. R. Silbar and M. M. Sternheim, Phys. Rev. C 6, 764 (1972).
- ²⁶S. Barshay, V. Rostokin, and G. Vagrado, Nucl. Phys. B59, 189 (1973).
- ²⁷J. P. Dedonder, Nucl. Phys. A180, 472 (1972).